Journal of Hydroscience and Hydraulic Engineering
Vol. 20, No.2 November, 2002, 131-140

ALTERNATE BARS FORMED ON BEDS WITH NON-UNIFORM SEDIMENT

By

H. Takebayashi

University of Tokushima, Minamijousanjima 2-1, Tokushima, Japan

and

S. Egashira

Ritsumeikan University, Nojihigashi 1-1-1, Kusatsu, Japan

SYNOPSIS

Longitudinal and transverse sediment sorting and its influence on the characteristics of bars on beds with cohesionless non-uniform sediment in straight open channels are studied by means of flume tests, numerical analysis and theoretical analysis. Findings show that the sediment sorting takes place on bars; finer sediment deposits around crests of bars and coarser sediment dominates in troughs. Furthermore, the wave height, wavelength and migration velocity of bars on beds with non-uniform sediment become smaller, shorter and faster, than those of bars formed on beds with uniform sediment.

INTRODUCTION

River training regulation works that enables both the restoration of natural riverine ecosystems and the flood control have become vital in recent years. In order to restore natural riverine ecosystems, habitats must be diversified. Size distribution of bed material and geometric characteristics of sand bars are important factors for the physical environment of plants, fishes, and animals. Size distribution of sediment should satisfy some conditions for the growth of vegetation or the spawning of fish [6, 10]. In addition, size distribution of sediment significantly affects the geometric and kinematic characteristics of bars [8]. Therefore, it is very important to clarify the dynamic characteristics of sand bars with heterogeneous bed materials.

Uniform bed material has been treated in most previous studies on the equilibrium geometric characteristics of sand bars. Hence, the effect of non-uniform sediment on geometric characteristics of bars is not understood completely. It is thought that longitudinal and transverse sediment sorting is responsible for the difference between geometring of with uniform and non-uniform sediment. Obviously, sediment sorting affects the local sediment discharge, resulting in different geometric characteristics.

In this study, the dynamic characteristics of sand bars on bed with non-uniform sediment is investigated focusing on the formative mechanism of alternate bars between confining banks of a straight open channel. Firstly, the longitudinal and transverse sediment sorting on bars is examined by means of flume tests, numerical analysis and theoretical analysis. Next, the effect of heterogeneous sediment on geometric characteristics of bars is analyzed, based on the results of flume tests and numerical analysis. Finally, the effect of sediment sorting on geometric characteristics of bars is examined using a linear bed stability analysis.

EXPERIMENTAL PROCEDURE

Experiments were carried out in a rectangular, straight open channel that is 15m in length and 30cm in width. Figure 1 shows size distribution of bed materials employed in the tests. Bed material A has a small standard deviation of 1.14 and is called

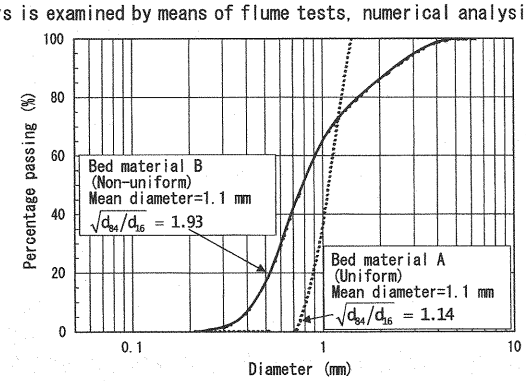

Fig. 1 Diameter distribution of sediment material employed for flume tests and numerical analysis

Table 1 Hydraulic conditions for flume tests and numerical analysis

	Bed material	Width/Depth	Bed slope	Non-dimensional shear stress	Froude number
Case 1	Uniform	25.0	1/71	0.100	1.22
Case 2	Non-uniform	25.0	1/71	0.100	1.22
Case 3	Uniform	25.4	1/50	0.143	1.50
Case 4	Non-uniform	25.4	1/50	0.143	1.50

uniform sediment for convenience. Bed material B is non-uniform sediment, the standard deviation of which is 1.93. Experimental conditions are shown in Table 1. Four cases, in which aspect ratios were almost the same, were conducted in different conditions concerning the bed material and non-dimensional bed shear stress. Alternate bars were expected to form in all cases according to the criterion of Kuroki and Kishi [5]. Initial bed geometry was flat. Water and sediment were supplied at a constant rate from the upstream end. Migration velocity of sand bars was measured by observation as well as by videotape. Bed geometry was measured after stopping the water supply. Bed material was collected from the surface layer, whose the thickness was equivalent to the maximum sediment diameter. Experiments were conducted until bars approached equilibrium state (about 30min.)

NUMERICAL METHOD

Depth integrated governing equations of momentum conservation and mass continuity, are employed for the numerical analysis.

$$\frac{\partial h}{\partial t} + \frac{\partial}{\partial x}(uh) + \frac{\partial}{\partial y}(vh) = 0 \tag{1}$$

$$\frac{\partial u}{\partial t} + u\frac{\partial u}{\partial x} + v\frac{\partial u}{\partial y} = -g\frac{\partial}{\partial x}(h + z_b) - \frac{\tau_x}{\rho h} + \frac{1}{h}\left[\frac{\partial}{\partial x}(h\sigma_{xx}) + \frac{\partial}{\partial y}(h\tau_{yx})\right] \tag{2}$$

$$\frac{\partial v}{\partial t} + u\frac{\partial v}{\partial x} + v\frac{\partial v}{\partial y} = -g\frac{\partial}{\partial y}(h + z_b) - \frac{\tau_y}{\rho h} + \frac{1}{h}\left[\frac{\partial}{\partial x}(h\tau_{xy}) + \frac{\partial}{\partial y}(h\sigma_{yy})\right] \tag{3}$$

where h is the water depth, u and v are the velocity components in the x and y directions respectively, z_b is the bed elevation, τ_x and τ_y are the bottom shear stresses in the x and y directions respectively, and σ_{xx}, τ_{yx}, τ_{xy} and σ_{yy} are the depth-averaged turbulence stresses. In order to evaluate the sediment discharge vector, velocity components at the bed surface are evaluated by using the curvature of streamline [2]. The sediment transport rate is evaluated by means of the Ashida-Michiue's formula [1], and the influence of local bed inclination on sediment transport rate and its direction are estimated by means of Hasegawa's formula [3]. Grain size distribution is estimated by using the following equation [4]:

$$E_m\frac{\partial f_{mi}}{\partial t} + f_{mi}\frac{\partial z_b}{\partial t} + \frac{1}{1-\lambda}\left(\frac{\partial q_{bxi}}{\partial x} + \frac{\partial q_{byi}}{\partial y}\right) = 0 \tag{4}$$

where f_{mi} denotes the concentration of sediment of size class-i in the exchange layer which is a thin bed surface layer exchanging bed material, E_m is the thickness of the exchange layer, q_{bxi} and q_{byi} are the sediment transport rates of size class-i in the x and y directions respectively, and λ is the porosity of bed sediment. The flow on alternate bars exhibits mixed sub- and super-critical flow. Hence the equations are discretized by using the TVD-MacCormack scheme.

The flow domain to be analyzed consists of a rectangular, straight open channel that is 15m in length and 30cm in width. Water is supplied at a constant rate from the upstream end. A small cubic disturbance, the heights of which is one-third the height of the initial uniform flow depth and one-fifth the flume width, is mounded on the upstream bed surface using bed material. Although several disturbance types are employed in our calculation, they do not affect the phenomena discussed in this paper. Hydraulic conditions used for the analysis are also shown in Table 1.

METHOD OF STABILITY ANALYSIS

A bed stability analysis is performed for flow in a straight open channel with rigid banks. The basic equations used for the analysis are the same as those for numerical analysis. The shear stress σ_{xx}, τ_{yx}, τ_{xy} and σ_{yy} in momentum conservation equations for water and unsteady terms of water flow, however, are not considered.

The following non-dimensional variables are introduced here:

$$\bar{x}=x/h_0\ ,\quad \bar{y}=y/h_0\ ,\quad \bar{t}=tu_0/h_0\ ,\quad \bar{u}=u/u_0\ ,\quad \bar{v}=v/u_0\ ,\quad \bar{h}=h/h_0\ ,\quad \bar{\tau}_x=\tau_x/(\rho g h_0 S)\ ,$$

$$\bar{\tau}_y=\tau_y/(\rho g h_0 S)\ ,\quad \bar{z}_b=z_b/h_0\ ,\quad F=u_0/\sqrt{gh_0}\ ,\quad \bar{E}_m=E_m/h_0\ ,\quad \bar{q}_{bxi}=q_{bxi}/q_{bp0}\ ,\quad \bar{q}_{byi}=q_{byi}/q_{bp0}\ ,$$

$$\bar{f}_{mi}=f_{mi}/f_{m0}\ ,\quad \bar{d}_m=d_m/d_{m0}\ ,\quad \bar{d}_i=d_i/d_{m0}\ ,\quad \bar{\tau}_{*i}=\tau_{*i}/\tau_{*0}$$

where the subscript 0 denotes the value of basic unperturbed flow, the superscriptions − denotes the normalized value, S is the bed slope, $q_{bpi}\left(=\sqrt{sgd_i^3}\Phi_i\right)$ is the sediment discharge of size class-i in the exchange layer, s is the specific weight of sand in water, ρ is the mass density of water, g is the acceleration due to gravity, Φ_i is the sediment discharge function of size class-i, d_m is the mean diameter of sediment, d_i is the sediment diameter of size class-i, $\tau_{*i}\left(=u_*^2/(sgd_i)\right)$ is the non-dimensional shear stress normalized by sediment size d_i, u_* is the friction velocity.

Furthermore, after perturbing the basic state, the following representation of the flow and the grain size distribution are introduced:

$$\bar{u}=1+\tilde{u}\ ,\quad \bar{v}=\tilde{v}\ ,\quad \bar{h}=1+\tilde{h}\ ,\quad \bar{\tau}_x=1+\tilde{\tau}_x\ ,\quad \bar{\tau}_y=\tilde{\tau}_y\ ,\quad \bar{z}_b=\tilde{z}_b\ ,$$

$$\bar{q}_{bxi}=\left(1+\tilde{q}_{bxpi}\right)\left(1+\tilde{f}_{mi}\right)=1+\tilde{q}_{bxpi}+\tilde{f}_{mi}\ ,\quad \bar{q}_{byi}=\tilde{q}_{bypi}\left(1+\tilde{f}_{mi}\right)=\tilde{q}_{bypi}\ ,\quad \bar{f}_{mi}=1+\tilde{f}_{mi}\ ,$$

$$\bar{d}_m=1+\tilde{d}_m\ ,\quad \bar{\tau}_{*i}=1+\tilde{\tau}_{*i}$$

where the superscription $\sim$ denote the value of perturbed flow. These quantities are substituted into the Equations (1) to (4) and the equations are linearized as follows:

$$\frac{\partial}{\partial\bar{x}}\left(\tilde{u}+\tilde{h}\right)+\frac{\partial\tilde{v}}{\partial\bar{y}}=0 \tag{5}$$

$$F^2\frac{\partial\tilde{u}}{\partial\bar{x}}+I\left(\tilde{\tau}_x-\tilde{h}\right)+\frac{\partial}{\partial\bar{x}}\left(\tilde{h}+\tilde{z}_b\right)=0 \tag{6}$$

$$F^2\frac{\partial\tilde{v}}{\partial\bar{x}}+I\tilde{\tau}_y+\frac{\partial}{\partial\bar{y}}\left(\tilde{h}+\tilde{z}_b\right)=0 \tag{7}$$

$$\bar{E}_m\frac{\partial\tilde{f}_{mi}}{\partial\bar{t}}+\frac{\partial\tilde{z}_b}{\partial\bar{t}}+A_{si}\left(\frac{\partial\tilde{q}_{bxpi}}{\partial\bar{x}}+\frac{\partial\tilde{f}_{mi}}{\partial\bar{x}}+\frac{\partial\tilde{q}_{bypi}}{\partial\bar{y}}\right)=0 \tag{8}$$

$$\tilde{\tau}_x=2\tilde{u}-2q\tilde{h}-2q\tilde{d}_m\ ,\quad \tilde{\tau}_y=\tilde{v} \tag{9}$$

$$\sum_{i=1}^{n}\bar{d}_i f_{mi0}\tilde{f}_{mi}=\tilde{d}_m\ ;\quad \sum_{i=1}^{n}\tilde{f}_{mi}f_{mi0}=0 \tag{10}$$

$$\tilde{q}_{bxpi}=\tau_{*i0}\tilde{\tau}_{*i}\frac{1}{\Phi\left(\tau_{*i0}\right)}\frac{\partial\Phi\left(\tau_{*i}\right)}{\partial\tau_{*i}}=\frac{3}{2}\frac{\tau_{*i0}}{\tau_{*i0}-\tau_{*ci}}\tilde{\tau}_{*i}\ ;\quad \tilde{q}_{bypi}=\tilde{v}-\sqrt{\frac{1}{\mu_k\mu_s}\frac{\tau_{*ci}}{\tau_{*i0}}}\frac{\partial\tilde{z}_b}{\partial\bar{y}} \tag{11}$$

$$\tilde{\tau}_{*i}=\tilde{\tau}_x \tag{12}$$

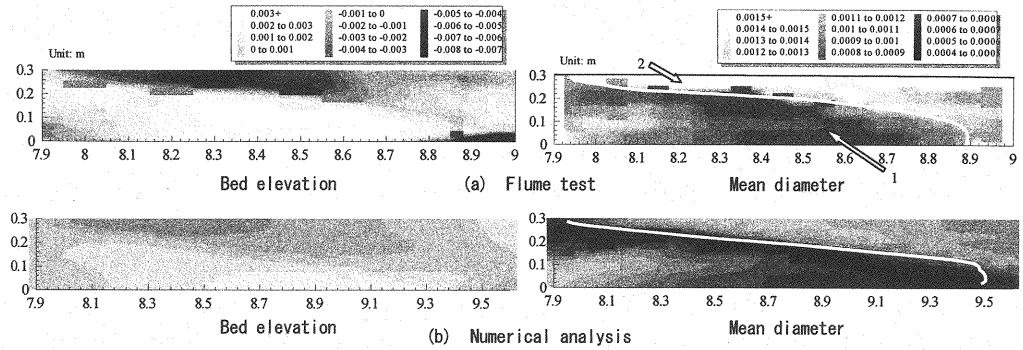

Fig. 2 Plane distribution of bed elevation and mean diameter (Case 1)

where $q = 2.5\Big/\left\{6.0 + 2.5\ln\left(\frac{h_0}{2d_{m0}}\right)\right\}$, $A_{si} = q_{bpi0}\Big/\left[(1-\lambda)u_0 h_0\right]$, τ_{*ci} is the non-dimensional critical shear stress for sediment size d_i, μ_k is the coefficient of dynamic friction, μ_s is the coefficient of static friction, n is the number of classification for sediment size. Linearity of the problem allows us to perform a normal mode analysis of perturbations by assuming

$$\left(\tilde{z}_b, \tilde{u}, \tilde{h}, \tilde{\tau}_x, \tilde{d}_m, \tilde{q}_{bxpi}, \tilde{f}_{mi}\right) = \left(\hat{z}_b, \hat{u}, \hat{h}, \hat{\tau}_x, \hat{d}_m, \hat{q}_{bxpi}, \hat{f}_{mi}\right) e^{ik(\bar{x}-\bar{c}\bar{t})}\cos\left(l\bar{y}\right) \tag{13}$$

$$\left(\tilde{v}, \tilde{\tau}_y, \tilde{q}_{bypi}\right) = \left(\hat{v}, \hat{\tau}_y, \hat{q}_{bypi}\right) e^{ik(\bar{x}-\bar{c}\bar{t})}\sin\left(l\bar{y}\right) \tag{14}$$

where the superscription ^ denote the non-dimensional amplitude of perturbation. The non-dimensional forms of the basic equations are as follows:

$$\begin{pmatrix} ik & l & 0 & ik & 0 & 0 & \cdots & 0 \\ ikF^2 + 2S & 0 & ik & ik - S - 2\eta S & -2\eta S & 0 & \cdots & 0 \\ 0 & ikF^2 + S & -l & -l & 0 & 0 & \cdots & 0 \\ 0 & 0 & 0 & 0 & -1 & \bar{d}_1 f_{m10} & \cdots & \bar{d}_n f_{mn0} \\ 0 & 0 & 0 & 0 & 0 & f_{m10} & \cdots & f_{mn0} \\ M_{11} & M_{12} & M_{13} & M_{14} & M_{15} & N_1 & \cdots & 0 \\ \vdots & \vdots & \vdots & \vdots & \vdots & \vdots & \ddots & \vdots \\ M_{n1} & M_{n2} & M_{n3} & M_{n4} & M_{n5} & 0 & \cdots & N_n \end{pmatrix} \begin{pmatrix} \hat{u} \\ \hat{v} \\ \hat{z}_b \\ \hat{h} \\ \hat{d}_m \\ \hat{f}_{m1} \\ \vdots \\ \hat{f}_{mn} \end{pmatrix} = 0 \tag{15}$$

where k (=$\pi h_0/L$) and l (=$\pi h_0/B$) are the longitudinal and transverse wave numbers respectively, L is the half wavelength, B is the channel width, $M_{i1} = 2ikA_{si}\alpha_i$, $M_{i2} = lA_{si}$, $M_{i3} = l^2 A_{si}\beta_i - ik\bar{c}$, $M_{i4} = -2ik\eta A_{si}\alpha_i$, $M_{i5} = -2ik\eta A_{si}\alpha_i$, $N_i = -ik\bar{c}\bar{E}_m + ikA_{si}$, $\alpha_i = \frac{3}{2}\frac{\tau_{*i0}}{\tau_{*i0} - \tau_{*ci}}$, $\beta_i = \sqrt{\frac{1}{\mu_k\mu_s}\frac{\tau_{*ci}}{\tau_{*i0}}}$, $\bar{c}$ is the complex migration velocity. The n-th order equation of $\bar{c}$ will be obtained by setting the determinant of the coefficient matrix of Equation (15) to 0. A value of $\bar{c}$ which is almost equivalent to the complex migration velocity of bars on the uniform sediment bed is chosen as the complex migration velocity of sand bars on beds with non-uniform sediment from n-solutions of $\bar{c}$, because the $\bar{c}$ is thought to derive from instability of bed elevation, which is the most focus of this analysis. It is thought that the others $\bar{c}$ originate in other phenomena (ex. sediment sorting waves). The subsequent analytical procedure is similar to the one that is used for the uniform sediment bed [5].

SEDIMENT SORTING ON BED SURFACE

Transverse and longitudinal distribution of mean sediment diameter and bed elevation obtained from flume

Table 2 Ratio of geometric and migration characteristic values of bars between uniform and non-uniform sediment beds

	Ratio of wave height (Non-uniform/Uniform)		Ratio of wavelength (Non-uniform/Uniform)		Ratio of migration velocity (Non-uniform/Uniform)	
	Flume test	Computation	Flume test	Computation	Flume test	Computation
Case 1 & Case 2	0.94	0.71	0.97	0.77	1.31	1.22
Case 3 & Case 4	0.59	0.55	0.82	0.68	1.24	1.27

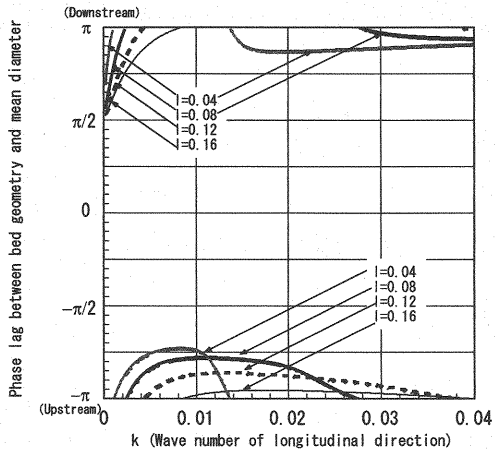

Fig. 3 Phase lag between bed geometry and mean diameter (Bed slope=1/50, Non-dimensional shear stress=0.143, l: Wave number of transverse direction)

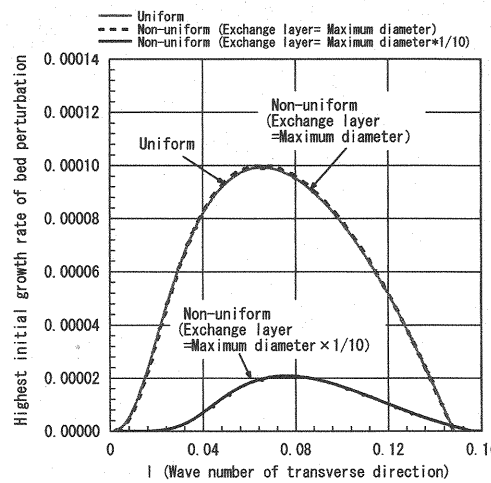

Fig. 4 Initial growth rate of bed perturbation along dominant wave number of longitudinal direction (Bed slope=1/50, Non-dimensional shear stress=0.143)

tests are shown in Figure 2 (a). The white solid lines denote the bar edges. Sediment particles are redistributed so that there are fine ones around crests (arrow 1) and coarse ones in troughs (arrow 2), respectively, because more fine particles are transported from troughs to crests than coarse sand. Transverse and longitudinal distribution of the mean sediment diameter and bed elevation obtained from the numerical analysis is shown in Figure 2 (b). The mean sediment diameter is fine around crests and coarse in troughs. The distribution range of the mean diameter obtained from numerical analysis, however, is narrower than the results obtained from the flume tests. The discrepancy between the experimental and numerical results is attributed to the fact that the bed geometry is not reproduced well numerically due to the unsuitable estimation of the exchange layer thickness. These problems will be examined in our future studies.

Figure 3 shows the spatial phase lag of sediment mean diameter relative to the bed geometry obtained from the linear bed stability analysis. The phase lag $k\theta$ ranges in the regions $\pi/2<k\theta<\pi$ and $-\pi<k\theta<-\pi/2$. This finding suggests that sand particles become finer around the crests and coarser in the troughs. This tendency of sediment size distribution is obtained from the flume tests and from the numerical analysis.

GEOMETRIC AND MIGRATION CHARACTERISTICS OF BARS

Table 2 summarizes wave height, wavelength and migration velocity of sand bars on beds with non-uniform sediment. The values are divided respectively by the corresponding values on beds with uniform sediment. Some of the characteristic values in both experimental and numerical results are less than unity, which means that the wave height and wavelength for non-uniform sediment are smaller than those for uniform sediment. On the other hand, the migration velocity is over unity and faster than that in the uniform sediment cases. Furthermore, such differences of characteristic values between non-uniform and uniform sediment increase with non-dimensional shear stress. In the next section the producing mechanism of the differences between the characteristics of bars for non-uniform and uniform sediment will be discussed.

Wave height

It is supposed that sediment sorting changes lateral and longitudinal distribution of sediment discharge

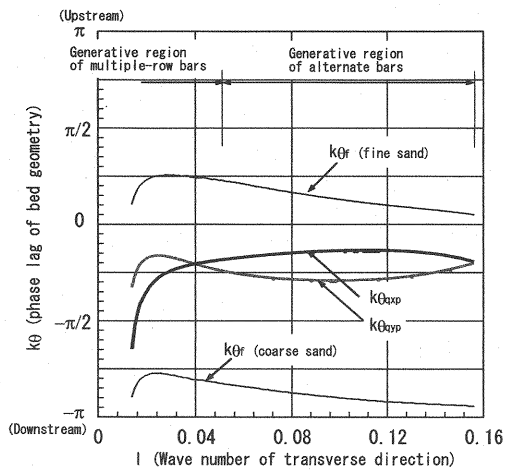

Fig. 5 Phase lag between bed geometry and specific terms in Eq. 16 (Bed slope=1/50, Non-dimensional shear stress=0.143)

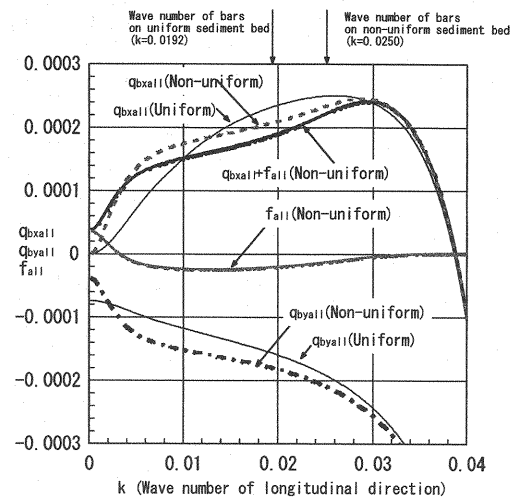

Fig. 6 Differences of the sum of specific terms in Eq. 16 between uniform and non-uniform sediment beds (Bed slope=1/50, Non-dimensional shear stress=0.143)

and suppresses deposition on crests and erosion in troughs, resulting in low wave height. To understand the effect of sediment sorting on wave height of bars, the initial growth rate of infestimal bed perturbation is investigated in terms of linear bed stability analysis. Figure 4 shows the initial growth rate of bed perturbation obtained from the analysis for uniform and non-uniform sediment. Herein, in order to clarify the effect of sediment sorting on the growth rate, calculations are conducted for two cases of exchange layer thickness; One is the same depth as maximum sediment size and the other is one-tenth the maximum sediment size. As shown in this figure, no significant difference is found in the initial growth rate between the results of the uniform sediment case and that of the non-uniform sediment case with a thick exchange layer. The reason for this is that temporal change of mean diameter is much slower than that of bed geometry under this condition. In comparison to these, the growth rate in the case of a thin exchange layer is predicted to be very small. This finding suggests the possibility that development of sediment sorting suppresses wave height. In the following analysis, the thin exchange layer is employed in order to clarify the effect of sediment sorting on geometric and migration characteristics of bars.

The initial growth rate of bed perturbation on beds with non-uniform sediment is expressed by the following linear bed stability analysis:

$$kc_I = -\sum_{i=1}^{n} f_{i0} A_{si} \left[\left|q_{bxpi}\right| k \sin\left(k\theta_{qxpi}\right) + \left|f_i\right| k \sin\left(k\theta_{fi}\right) + \left|q_{bypi}\right| l \cos\left(k\theta_{qypi}\right) \right] \qquad (16)$$

where c_I is the imaginary part of the non-dimensional migration velocity of bars, kθ is the phase lag relative to the bed geometry, $|\ |$ denotes the amplitude of perturbation with respect to the bed geometry. The value n=1 in Equation (16) indicates a uniform sediment condition.

Equation (16) indicates that bed perturbations are stable in the range of the phase lags $0<k\theta<\pi$ for $|q_{bxpi}|$ and $|f_i|$, and $-\pi/2<k\theta<\pi/2$ for $|q_{bypi}|$. These phase lags along dominant longitudinal wave numbers are depicted in Figure 5. The amplitude of bed perturbation develops in the range of phase lag $-\pi<k\theta_{qxp}<0$. On the other hand, the amplitude is suppressed in the range of phase lag $-\pi/2<k\theta_{qyp}<\pi/2$. These results are the same as those for the uniform sediment [5]. Next, let us separate the phase lag $k\theta_f$ into fine and coarse parts and then discuss. As shown in Fig. 5, the phase lag of coarse sand ranges $-\pi<k\theta_f<0$ and thus enhances the development of bed perturbation. On the other hand, the phase lag of fine sand ranges $0<k\theta_f<\pi$ and thus suppresses the amplitude of bed perturbation. These results suggest that fine sand contributes to the suppression of wave height in the non-uniform sediment case.

Figure 6 shows the sums of specific terms in Eq. 16 which are defined as follows:

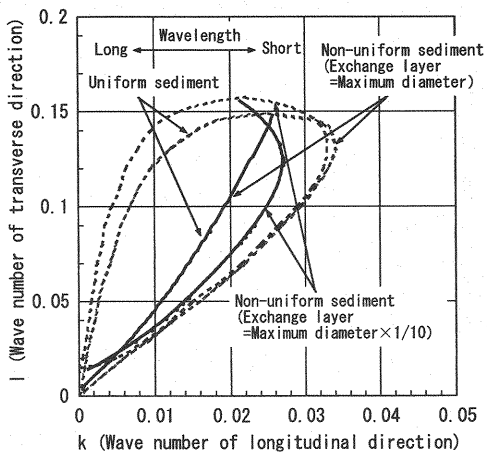

Fig. 7 Difference of wavelength between uniform and non-uniform sediment beds (Solid and broken lines indicate dominant longitudinal wave numbers and neutral line between stable and unstable bed perturbation respectively. Bed slope= 1/50, Non-dimensional shear stress = 0.143)

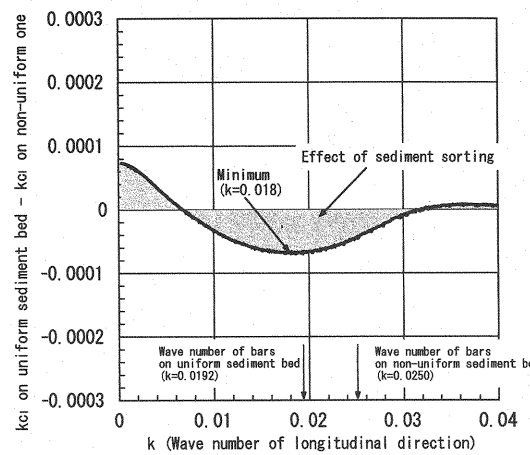

Fig. 8 Difference of initial growth rate of bed perturbation between uniform and non-uniform sediment beds (0 in the vertical axis indicates no differences. Bed slope= 1/50, Non-dimensional shear stress=0.143)

$$q_{bxall} = \sum_{i=1}^{n} f_{i0} A_{si} \left| q_{bxpi} \right| k \sin\left(k\theta_{qxpi}\right) ; \quad f_{all} = \sum_{i=1}^{n} f_{i0} A_{si} \left| f_i \right| k \sin\left(k\theta_{fi}\right) \tag{17}$$

$$q_{byall} = \sum_{i=1}^{n} f_{i0} A_{si} \left| q_{bypi} \right| \cos\left(k\theta_{qypi}\right)$$

The sum of q_{bxall} and f_{all} indicates longitudinal sediment discharge. Their small absolute values refer to a decrease in the rate of change of longitudinal sediment transport discharge at crests. Figure 6 suggests that the changing rate of longitudinal sediment discharge in non-uniform sediment is suppressed in comparison to that in uniform sediment. On the other hand, the absolute value of q_{byall} is larger than that of the uniform sediment cases. The value, however, is negative. Therefore, it can be said that not only the deformation of longitudinal sediment discharge distribution but also that of the transverse one suppresses the initial growth rate of bed perturbation of beds with non-uniform sediment. Herein, these differences of q_{bxall} and q_{byall} between uniform and non-uniform sediment are produced by the difference of the flow field depending on the spatial distribution of mean sediment diameter. On the other hand, f_{all} consists of the spatial distribution of the concentration of sediment. It is apparent that sediment sorting is responsible for these differences.

Wavelength

The mechanism shortening wavelength of bars on beds with non-uniform sediment is examined below, based the results obtained by means of linear bed stability analysis. The wavelength with the highest initial growth rate of bed perturbation, which is regarded as an equilibrium wavelength, will be the focus of discussion.

Figure 7 shows calculated lines for the highest initial growth rate (solid lines). Neutral curves between stable and unstable bed perturbation are also shown in Fig. 7 (broken lines). Bars will be formed within of the neutral curves. According to these results, wave number (wavelength) in the longitudinal direction of the non-uniform sediment case is larger (smaller) than that of the uniform case. The wavelength tends to shift to a length with a small suppressive effect of sediment sorting on the initial growth rate, because a wavelength with highest initial growth rate of bed perturbation is regarded as an equilibrium wavelength. Figure 8 shows the difference of the initial growth rate of bed perturbation on between uniform and non-uniform sediment. The negative values in Fig. 8 show suppression of the initial growth rate of bed perturbation. The suppressive effect of sediment sorting on the initial growth rate varies with the longitudinal wave number, and is large around the wavelength of uniform sediment (k=0.0192). Consequently, the wavelength shifts to the shorter value; k=0.0250, which has the highest initial growth rate of bed perturbation on beds with non-uniform sediment.

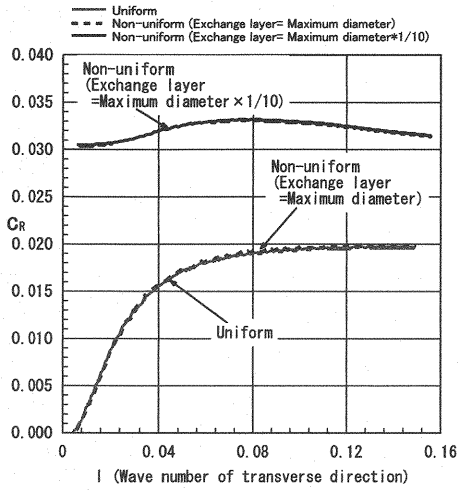

Fig. 9 Non-dimensional migration velocity along dominant wave number of longitudinal direction (Bed slope=1/50, Non-dimensional shear stress=0.143)

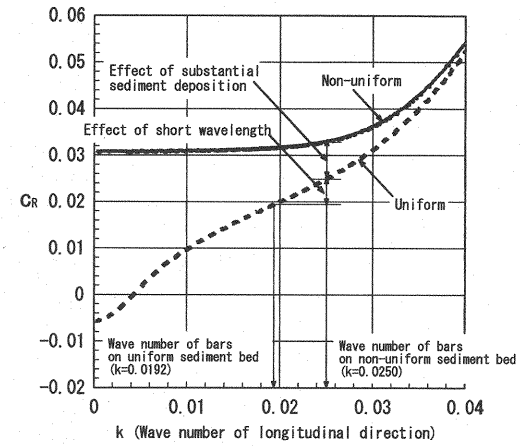

Fig. 10 Difference of non-dimensional migration velocity (c_R) of bars between uniform and non-uniform sediment beds (Bed slope=1/50, Non-dimensional shear stress=0.143)

Migration velocity

Migration velocity of bars is expressed in the following linear bed stability analysis as follows.

$$c_R = \sum_{i=1}^{n} f_{i0} A_{si} \left[\left| q_{bxpi} \right| \cos\left(k\theta_{qxpi} \right) + \left| f_i \right| \cos\left(k\theta_{fi} \right) + \left| q_{bypi} \right| \Big/ k \sin\left(k\theta_{qypi} \right) \right] \tag{18}$$

Eq. 18 indicates that bed perturbations migrate downstream on the phase lags $-\pi/2<k\theta<\pi/2$ for $\left|q_{bxpi}\right|$ and $\left|f_i\right|$, $-\pi<k\theta<0$ for $\left|q_{bypi}\right|$. Figure 5 indicates that the phase lag, $k\theta_{qxp}$, falls in the range $-\pi<k\theta_{qxp}<0$ and contributes to the downstream bar migration. Furthermore, the phase lag, $k\theta_{qyp}$, falls in the range $-\pi<k\theta_{qyp}<0$ and enhances downstream bar migration, too. Next, $k\theta_f$ is separated into finer and coarser sediment phase lags. The phase lag, $k\theta_f$, of coarse sediment falls in the range $-\pi<k\theta<-\pi/2$, $\pi/2<k\theta<\pi$ and suppresses bar migration. On the other hand, $k\theta_f$ of fine sediment falls in the range $-\pi/2<k\theta<\pi/2$ and contributes to the downstream bar migration. In order to migrate downstream, sand particles should deposit on the downstream side of the bar crest. Figure 9 shows the migration velocity of bars obtained from the linear bed stability analysis. It is revealed that migration velocity of bars increases on the bed where sediment sorting is well developed. These findings imply that high migration velocity of bars on beds with non-uniform sediment is induced by a large amount of deposition of fine sediment.

A previous study [7] suggests that sand bars with a short wavelength migrate faster than those with a long wavelength. As discussed in the previous section of this paper, the wavelength of bars in the non-uniform sediment case is shorter than that in the uniform case. Hence, it is thought that the migration velocity of bars in the case of non-uniform sediment increases due to a short wavelength. Furthermore, transported sediment volume available for bar migration on non-uniform sediment bed is the same as that for bar migration on the uniform one even though wave height of bars on non-uniform sediment bed is lower than that of those on the uniform one [9]. Consequently, these two effects, short wavelength and substantial sediment deposition consumed for bar migration, are thought to be the reason why migration velocity in the non-uniform sediment increases. It is possible to regard the two effects as one, because sediment sorting causes both. In order to clarify the mechanism of fast bar migration on the non-uniform sediment bed, these effects are examined separately here. The change of equilibrium migration velocity of bars with longitudinal wave number is drawn in Figure 10. Migration velocity increases with the increase in longitudinal wave number (decrease in wavelength). On the other hand, substantial sediment deposition causes the difference of migration velocity between the uniform and non-uniform sediment and accelerates bar migration. As a result, migration velocity of bars in the non-uniform sediment increases due to the two effects as shown in Fig. 10.

CONCLUSION

Geometric and kinematic characteristics of alternate bars with non-uniform sediment formed between confining banks of a straight open channel are examined based on flume tests and numerical and stability analyses. The findings of this study are summarized as follows:

(1) Sediment sorting takes place on bars with non-uniform sediment. Mean sediment diameter becomes finer around crests of bars and coarser in troughs, respectively.

(2) The wave height of bars with non-uniform sediment is smaller than the one that a uniform sediment, because sediment sorting decreases the rate of change of longitudinal sediment discharge, and increases the transverse change rate at bar crests.

(3) The equilibrium wavelength of bars with non-uniform sediment is shorter than that with uniform sediment because the initial growth rate of bed perturbation with a long wavelength is more suppressed than the one with a short wavelength.

(4) Migration velocity increases with the decreasing wavelength. Furthermore, the volume of transported sediment available for bar migration on the non-uniform sediment bed is the same as that for bar migration on the uniform bed even though the wave height of the bars on the non-uniform sediment bed is lower than the wave height of the bars on the uniform bed. These two effects amplify the equilibrium migration velocity of bars in the case of non-uniform sediment.

ACKNOWLEDGEMENT

The flume experiments and data processing were performed with the assistance of Mr. Hasegawa, a graduate student of Ritsumeikan University (currently, Civil Engineering Research Laboratory Foundation), and Miss Akahata, an undergraduate student of Ritsumeikan University (currently, Taiseikikou Co. Ltd.). The authors are grateful for their support.

REFFERENCES

1. Ashida, K. and Michiue, M. : Study on hydraulic resistance and bed-load transport rate in alluvial streams, Proc. of JSCE, No. 206, pp. 59-69, 1972 (in Japanese).
2. Engelund, F. : Flow and Bed topography in channel bends, Jour. of Hy. Div. ASCE, Vol. 100, No. HY11, 1974.
3. Hasegawa, K: Bank-erosion discharge based on a nonequilibrium theory, Trans. of JSCE, 13, pp. 202-204, 1981.
4. Hirano, M. : Studies on variation and equilibrium state of a river composed of nonuniform material, Proc. of JSCE, No. 207, pp. 51-60, 1972 (in Japanese).
5. Kuroki, M. and Kishi, T. : Regime criteria on bars and braids in alluvial straight channels, Proc. of JSCE, No. 342, pp. 87-96, 1984 (in Japanese).
6. Kamada, M., Kori, M., Mihara, S. and Okabe, T. : Distribution of *Salix* spp. and *Elaeagnus umbellata* communities relation to their stand characteristics on bars in Yoshino River, Shikoku, Japan, Environmental Systems Research, Vol. 27, pp. 331-337, 1999 (in Japanese).
7. Nagata, N., Muramoto, Y., Uchikura, Y, Hosoda, T., Yabe, M., Takada, Y. and Iwata, M : On the behavior of alternate bars under several kinds of channel conditions, Annual Journal of Hydraulic Engineering, JSCE, Vol. 43, pp. 743-748, 1999 (in Japanese).
8. Takahashi, F., Egashira S. and Yoshizumi, M. : The effect of non-uniform sediment on the geometric characteristics of sand bars, Kansai Chapter Proc. of Annual Conference of Civil Engineers, JSCE, II-68, 1995 (in Japanese).
9. Takebayashi H., Egashira S. and Jin H. S. : Numerical simulation of alternate bar formation, Proc. of 7th ISRS, pp. 733-738, 1998.
10. Tamai, N., Mizuno, N. and Nakamura, S. : Environmental River Engineering, Tokyo University Press, pp. 89-95, 1993 (in Japanese).

APPENDIX - NOTATION

The following symbols are used in this paper:

B = channel width;

$\bar{c}$ = complex migration velocity;

c_I = imaginary part of non-dimensional migration velocity of bars;

c_R = real part of non-dimensional migration velocity of bars;

d_i = sediment particle diameter of size class i;

d_m = mean diameter of sediment;

E_m = thickness of exchange layer;

F = Froude number;

f_{mi} = concentration of sediment of size class i in exchange layer;

g = acceleration due to gravity;

h = water depth;

i = sediment size class;

k $(=\pi h_0/L)$ = wave number in x direction;

kθ = phase lag relative to bed geometry;

l $(=\pi h_0/B)$ = wave number in y direction;

L = half wavelength;

n = total number of size classes of bed material;

q_{bpi} $(=\sqrt{sgd_i^3}\Phi_i)$ = sediment discharge of size class i divided by concentration of sediment of size class i in exchange layer;

q_{bxi}, q_{byi} = sediment transport rate of size class i in the x and y directions respectively;

s = specific weight of sand in water;

S = bed slope;

subscript 0 = value of basic unperturbed flow;

t = time;

u, v = velocity components in x and y directions respectively;

x, y = longitudinal and transverse Cartesian coordinates respectively;

z_b = bed elevation;

Φ_i = sediment discharge function of size class i;

λ = porosity of bed sediment;

μ_k = coefficient of dynamic friction;

μ_s = coefficient of static friction;

τ_x, τ_y = shear stress in x and y directions respectively;

τ_{*i} = non-dimensional shear stress of size class i;

τ_{*ci} = non-dimensional critical shear stress of size class i;

$\sim$ = value of perturbed flow;

$-$ = non-dimensional value;

$\hat{}$ = non-dimensional amplitude of perturbation; and

$|\ |$ = amplitude of perturbation with respect to bed elevation.

(Received December 14, 2001 ; revised March 25, 2002)